7

Freeboard Heat Transfer

We saw in Chapter 6 that the energy required to drive the direct-fired rotary kiln process is produced as a result of combustion, typically from fossil or waste fuel, in the freeboard. We also saw that the heat source to sustain the flame must come from heat transfer, hence the need to include enthalpy in the conservation equations. Heat transfer in the freeboard is more than just to sustain combustion at the combustion zone; it involves the exchange of energy from the freeboard to the bed to carry out the material process operation. For a process to be efficient, we must get most of the energy into the material and later exhaust the rest. In addition to driving the process, heat transfer is also important for its control. Since the rates at which chemical reactions proceed are strong functions of temperature, controlling the temperature profiles in the freeboard is tantamount to controlling the bed process. Heat transfer in rotary kilns encompasses all the modes of transport mechanisms, that is, conduction, convection, and radiation. In the freeboard, radiation is believed to be the dominant mode of heat transfer constituting over 90 percent, primarily due to the large flame and curvature of the combustion chamber. Convection in the freeboard occurs as a function of the turbulent flow of gases and participates in the transfer of heat to the bed's free surface and the refractory wall in a manner similar to flow over heated plates. Convection also occurs in the interparticle interstices within the particulate bed. Heat is conducted from the freeboard to the outside environment through

the refractory wall and must overcome the resistances to heat flow through the composite walls of refractory materials to reach the outer kiln shell. Within the bed, heat transfer is by interparticle conduction, which, together with interparticle convection and radiation, form an effective conductance of heat through the particulate medium. In this chapter we will review classic heat transfer mechanisms and point out where the phenomenon comes into play in the freeboard of the rotary kiln. This will be followed, in Chapter 8, by similar treatment for the bed.

7.1 Overview of Heat Transfer Mechanisms

As we have mentioned virtually all the various modes of heat transfer, that is, conduction, convection, and radiation, occur in the kiln although each contribution may vary depending on the temperature and for that matter on the axial location or zone. Conduction and radiation are fundamental physical transfer mechanisms, while convection is really conduction as effected by fluid flow. Classical definitions have it that conduction is an exchange of energy by direct interaction between molecules of a substance subjected to temperature difference. Conduction can occur in gases, liquids, or solids but it normally refers to heat transfer within solid materials. Radiation, on the other hand, is a transfer of thermal energy in the form of electromagnetic waves emitted by atomic agitation at the surface of a body. Like all electromagnetic waves, for example, light, X-rays, microwaves, and so on, thermal radiation travels at the speed of light passing most easily through vacuum or nearly transparent gases such as oxygen or nitrogen. CO_2 and H_2O transmit a portion of thermal radiation. Radiation normally occurs between solid surfaces but does not require any contact or intervening medium. Radiation may also occur within some fluids or between these fluids and solid surfaces. Generally this mechanism is important only at elevated temperatures. Convection may be described as conduction in a fluid as enhanced by the motion of the fluid. It normally refers to heat transfer between a fluid and a solid surface.

Although the division of heat transfer into these modes oversimplifies the situation, it is adequate provided it is realized that all three modes possess some common features. Despite the fact that each mode

is represented by different types of equations they all reduce to the common form defined by the heat flux as

$$\text{Heat Flux} = \text{Driving Force} \div \text{Resistance}, \quad \text{or}$$
$$\text{Conductance} \times \text{Driving Force} \tag{7.1}$$

where the driving force is the temperature difference and the resistance is a measure of the material's ability to transport energy. We might note that the units for heat flux are

$$\frac{\text{Energy}}{\text{Area} \times \text{Time}}; \quad \text{for example,} \quad \frac{\text{kJ}}{\text{m}^2\text{s}} = \frac{\text{kW}}{\text{m}^2} \tag{7.2}$$

Since energy is the property of systems, that is, of mass or, more specifically, molecules, we might correctly expect similarities with other transport processes which involve the transport of molecules, for example, mass transfer and momentum transfer. Hence many process problems involve the transfer and conservation of mass, momentum, and heat as we saw in the description of reactive flow equations in the CFD approach.

7.2 Conduction Heat Transfer

In solid materials such as refractory walls or the shell of a rotary kiln the molecules form a rigid lattice structure. Although molecules do not migrate within the lattice, they possess internal energy in various forms, such as vibrational and rotational kinetic energy, which, in turn, are in proportion to the local temperature. If the material is not uniform in temperature, that is, if there is a temperature difference within the material, energy will be transferred by molecular interaction from the more energetic molecules in the region with higher temperature to the less energetic molecules in the region with lower temperature. The rate at which this energy transfer occurs depends both on the temperature gradient in the direction of transfer and on the modes of molecular interaction present in that particular material (thermal conductivity), that is, Fourier's law of heat conduction. Fourier's law states that the flux of energy or the heat flux by conduction across a plane normal to, for example, the x-axis (Figure 7.1) is proportional to the temperature gradient, that is,

$$q'' = -k\frac{\partial T}{\partial x} \quad \left[\frac{\text{kW}}{\text{m}^2}\right] \tag{7.3}$$

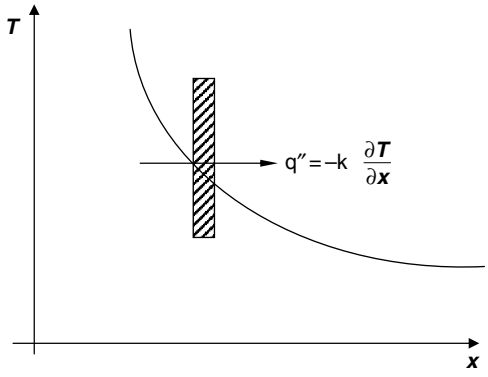

Figure 7.1 Fourier's definition of conduction heat transfer.

By combining Fourier's law and the requirements of energy conservation, one can derive the governing equation for conduction when the temperature varies in only one coordinate, for example, the x-axis. We do that by considering a control volume of infinitesimal size in the solid lattice (Figure 7.2).

For a surface with area $dy \cdot dz$ at coordinate $x - dx/2$,

$$q_{x-dx/2,t} = q_{x,t} + \frac{\partial}{\partial x}(q)_{x,t}\left(-\frac{dx}{2}\right)$$
$$= -\left[k dy dz \frac{\partial T}{\partial x}\right]_{x,t} + \frac{\partial}{\partial x}\left[-k dy dz \frac{\partial T}{\partial x}\right]_{x,t}\left(-\frac{dx}{2}\right) \qquad (7.4)$$

Similarly for the surface with area $dy \cdot dz$ at coordinate $x + dx/2$,

$$q_{x+dx/2,t} = -\left[k dy dz \frac{\partial T}{\partial x}\right]_{x,t} + \frac{\partial}{\partial x}\left[k dy dz \frac{\partial T}{\partial x}\right]_{x,t}\left(+\frac{dx}{2}\right) \qquad (7.5)$$

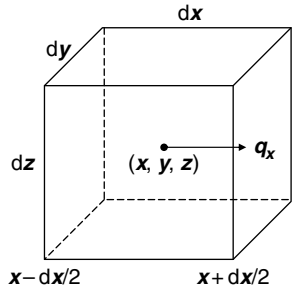

Figure 7.2 Control volume.

Adding Equations (7.4) and (7.5) gives the rate at which energy crosses into the control volume over the surfaces $x \pm \mathrm{d}x/2$

$$q_{CS,t} = \frac{\partial}{\partial x}\left[k\mathrm{d}y\mathrm{d}z\frac{\partial T}{\partial x}\right]_{x,t}\left(\frac{\mathrm{d}x}{2}+\frac{\mathrm{d}x}{2}\right)$$

$$q_{CS,t} = k\mathrm{d}x\mathrm{d}y\mathrm{d}z\frac{\partial^2 T}{\partial x^2} \tag{7.6}$$

For constant pressure processes the specific enthalpy h is the measure of the internal energy possessed by the material. The specific heat is related to the internal energy as

$$c_p = \left(\frac{\partial h}{\partial T}\right)_{p,T} \quad \Rightarrow \quad \mathrm{d}h = c_p\mathrm{d}T \tag{7.7}$$

Equation (7.7) can be equated to the rate of energy accumulation in the control volume as

$$\frac{\partial}{\partial t}\left(h\rho\mathrm{d}V\right) = \rho\mathrm{d}V\frac{\partial h}{\partial t} = \rho c_p\mathrm{d}x\mathrm{d}y\mathrm{d}z\frac{\partial T}{\partial t} \tag{7.8}$$

If there is no source term generating energy within the control volume, then the first law of thermodynamics requires energy conservation for which the rate of heat accumulation must equal the rate at which heat crosses into the control surfaces, that is, Equations (7.6) and (7.8) are equal

$$\frac{c_p\rho}{k}\frac{\partial T}{\partial t} = \frac{\partial^2 T}{\partial x^2} \tag{7.9}$$

If there is a source of heat within the control volume, then the heat of accumulation within the control volume must equal the rate at which heat crosses the control surfaces plus rate at which heat is evolved within the control volume (source of heat within, $\dot{q}$), that is,

$$\frac{c_p\rho}{k}\frac{\partial T}{\partial t} = \frac{\partial^2 T}{\partial x^2} + \dot{q} \tag{7.10}$$

Equation (7.10) is the representation of a transient (unsteady-state), one-dimensional heat conduction that must be satisfied at all points within the material. The combination of properties, $\alpha = k/c_p\rho$, which has units of m^2/s, is known as the thermal diffusivity, and is an important parameter in transient conduction problems. α is a measure of the efficiency of energy transfer relative to thermal inertia. For a given time under similar heating conditions, thermal effects will

penetrate farther through material of relatively high diffusivity. That is to say that heat will penetrate faster in metals, for example, aluminum with $\alpha \approx 1 \times 10^{-4}\,\mathrm{m^2/s}$, than through a fireclay refractory brick with $\alpha \approx 1 \times 10^{-7}\,\mathrm{m^2/s}$, but variations in temperature during heating will be less in aluminum.

Following the same analysis, the transient conduction for a multidimensional temperature field would be

$$\frac{c_p \rho}{k}\frac{\partial T}{\partial t} = \frac{\partial^2 T}{\partial x^2} + \frac{\partial^2 T}{\partial y^2} + \frac{\partial^2 T}{\partial z^2} + \dot{q} \tag{7.11}$$

and for steady-state conduction with no heat source, the equation reduces to what is known as the Laplace equation, that is,

$$\frac{\partial^2 T}{\partial x^2} + \frac{\partial^2 T}{\partial y^2} + \frac{\partial^2 T}{\partial z^2} = 0 \tag{7.12}$$

Equation (7.12) is the form that is required to solve for the temperature distribution in any rectilinear block of material as those encountered in the refractory linings of rotary kilns. Consider a section of a plane wall that is some distance from any edge or corner, for example, a refractory section in the freeboard with certain thickness, receiving heat from the freeboard gas (Figure 7.3).

For this case, the Laplace equation will take on the very simple form, $\frac{\partial^2 T}{\partial x^2} = 0$, which has a general solution, $T(x) = C_1 x + C_2$. If we have temperature measurements for the boundaries such that

$$\text{at} \quad x = x_1, \; T = T_1$$
$$\text{at} \quad x = x_2, \; T = T_2$$

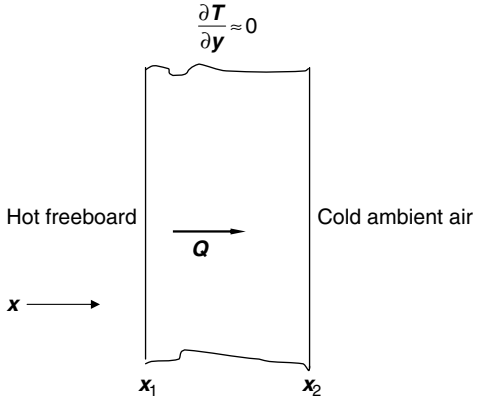

Figure 7.3 Conduction through a plane wall.

then the general solution yields a linear temperature distribution within the refractory lining at the location of interest as

$$T(x) = \frac{(T_2 - T_1)}{(x_2 - x_1)}x + T_1 \tag{7.13}$$

Equation (7.13) is the analytical solution yielding the distribution of temperature from which heat transfer by conduction through the wall can be established. The rate of heat transfer through the lining can be estimated by invoking the Fourier law as

$$Q = Aq'' = -kA\frac{(T_2 - T_1)}{(x_2 - x_1)} = \text{constant} \tag{7.14}$$

Although the local heat loss through a lining can be approximated by a plane slab, the global heat loss through a refractory lining in a rotary kiln is through a cylindrical surface. Nonetheless, the Laplace equation for a rectilinear control volume can be extended to a cylindrical control volume as well (Figure 7.4).

From Figure 7.4, conservation of energy requires that

$$\rho c_p \frac{\partial T}{\partial t} = \frac{1}{r}\frac{\partial}{\partial r}\left(rk\frac{\partial T}{\partial r}\right) + \frac{1}{r^2}\frac{\partial}{\partial \theta}\left(k\frac{\partial T}{\partial \theta}\right) + \frac{\partial}{\partial z}\left(k\frac{\partial T}{\partial z}\right) + \dot{q} \tag{7.15}$$

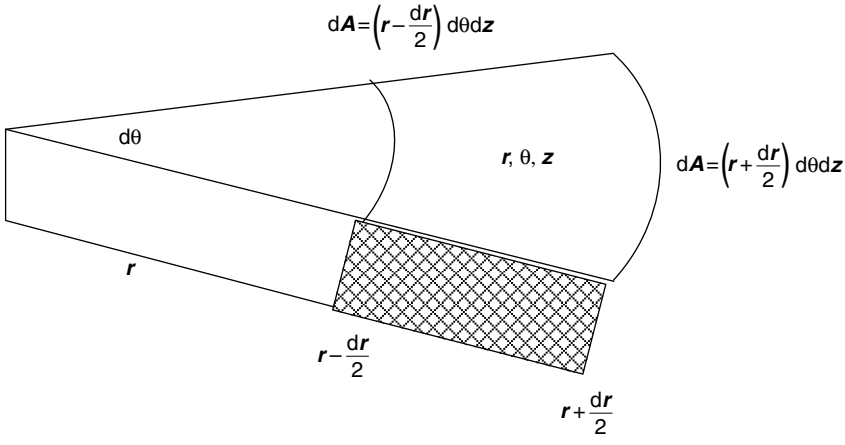

Figure 7.4 Cylindrical control volume for heat conduction.

and for steady state conduction within material of uniform conductivity, the equation reduces to the Laplace equation in cylindrical coordinates

$$\frac{\partial^2 T}{\partial r^2} + \frac{1}{r^2}\frac{\partial^2 T}{\partial \theta^2} + \frac{\partial^2 T}{\partial z^2} = 0 \tag{7.16}$$

For the specific case of one-dimensional steady-state heat transfer through a cylindrical wall, the Laplace equation reduces to

$$\frac{\mathrm{d}^2 T}{\mathrm{d}r^2} + \frac{1}{r}\frac{\mathrm{d}T}{\mathrm{d}r} = 0 \tag{7.17}$$

which, for the case of a refractory lining section a distance away from edges, presented earlier, has a specific solution,

$$T(r) = T_1 + (T_2 - T_1)\frac{\ln(r/r_1)}{\ln(r_2/r_1)}$$

or, with some rearrangement, gives the temperature distribution,

$$\frac{T(r) - T_1}{T_2 - T_1} = \frac{\ln(r/r_1)}{\ln(r_2/r_1)} \tag{7.18}$$

Equation 7.18 shows that unlike the rectilinear plane wall, the temperature distribution is not linear. The heat flux declines as r increases due to increasing area, $r\mathrm{d}\theta\mathrm{d}z$. Nonetheless, we can apply Fourier's law to this result to obtain an expression for the heat transfer rate through the wall of a pipe with length L or for that matter a rotary drum cylinder of length L as

$$Q = \frac{T_1 - T_2}{\dfrac{\ln(r_2/r_1)}{2\pi kL}} \tag{7.19}$$

7.3 Convection Heat Transfer

As mentioned earlier, convective heat transfer occurs between a solid surface and an adjacent moving fluid. The rate of heat transfer between a surface at temperature T_w and a fluid at T_f can be calculated from Newton's law of cooling, which is mathematically stated as

$$Q = hA(T_\mathrm{w} - T_\mathrm{f}) \tag{7.20}$$

The simplicity of Equation (7.20) should not obscure the complexity of determining h, the heat transfer coefficient which is a

complicated function of both flow and the thermophysical properties of the fluid, that is, viscosity, density, and their relationships such as the Reynolds number $\rho uL/\mu$, Prandtl number $\mu c_p/k$, the ratio of the momentum diffusivity (μ/ρ) to thermal diffusivity ($k/c_p\rho$), and so on. Convection problems are classified as (i) forced convection, where the fluid is induced by a fan, pump, and so on, or (ii) free convection, where the flow is driven by temperature induced density variations in the fluid, that is, buoyancy or a combination thereof. The study of convection heat transfer concerns the ways and means of calculating values for the convective coefficient, h. This involves solution of the Navier Stokes equations given previously in Chapter 6.

Some analytical solutions of boundary layer flows have been used to deduce the relationships between the heat transfer coefficient and the flow properties. For example, fluid flow over heated surfaces develops two boundary layer thicknesses, that is, the hydrodynamic boundary layer and the thermal boundary layer. When these two layers coincide, then, $Pr = 1$. For flow over a flat surface the condition of "no slip" at the wall suggests that the heat transfer in the fluid directly contacting the wall, that is, in the thin layer adjacent to the wall, occurs by pure conduction. Therefore the heat flux is given by

$$q'' = k_{\mathrm{f}} \left(\frac{\partial T}{\partial y} \right)_{y=0} = h\,(T_\infty - T_{\mathrm{w}}) \tag{7.21}$$

where

$$h = k_{\mathrm{f}} \left(\frac{\partial T}{\partial y} \right)_{y=0} \left(\frac{1}{T_\infty - T_{\mathrm{w}}} \right) \tag{7.22}$$

Like the dimensionless Reynolds number, the non-dimensional form of the heat transfer coefficient is defined by the Nusselt number, $Nu_x = hx/k_{\mathrm{f}}$ over the boundary layer. One correlation relating heat and flow over heated surfaces is

$$Nu_x = 0.322\, Re_x^{1/2} Pr^{1/3} \tag{7.23}$$

One can also integrate the local values of the Nusselt number to obtain the average value for a plate of length L as

$$Nu_x = 0.664\, Re_x^{1/2} Pr^{1/3} \tag{7.24}$$

There is also flow around heated bluff bodies and other complex surfaces for which modified forms of the Nusselt correlations have

been deduced. For rotary kiln applications, the convective component of the heat transfer is small and in most cases Equation (7.23) may suffice in estimating the convective heat transfer coefficient, h.

7.4 Conduction-Convection Problems

Conduction usually occurs in conjunction with convection, and if the temperatures are high, they also occur with radiation. In some practical situations where radiation cannot be readily estimated, convection heat transfer coefficients can be enhanced to include the effect of radiation. Combined conduction and convection led to the concept of thermal resistances, analogous to electrical resistances, which can be solved similarly.

We will now consider the problem of calculating the heat transfer from a hot fluid to a composite plane of refractory wall and through an outer steel shell.

1. Convection from the freeboard to the inside refractory surface will follow Newton's law of cooling as

$$q''_{\mathrm{g}} = h_{\mathrm{g}} \left(T_{\mathrm{g}} - T_{\mathrm{iR}} \right) \tag{7.25}$$

2. This is followed by one-dimensional steady state conduction through the refractory lining

$$q''_{\mathrm{R}} = k_{\mathrm{R}} \left(\frac{T_{\mathrm{iR}} - T_{\mathrm{Rs}}}{L_{\mathrm{R}}} \right) \tag{7.26}$$

3. The next step is one-dimensional steady state conduction through the steel shell

$$q''_{\mathrm{s}} = k_{\mathrm{s}} \left(\frac{T_{\mathrm{Rs}} - T_{\mathrm{sa}}}{L_{\mathrm{s}}} \right) \tag{7.27}$$

4. After leaving the shell, heat is transferred to the atmosphere by convection to the air at ambient temperature, that is,

$$q''_{\mathrm{a}} = h_{\mathrm{a}} \left(T_{\mathrm{sa}} - T_{\mathrm{a}} \right) \tag{7.28}$$

For steady-state conditions with no accumulation of energy within the wall or the gas

$$q''_{\mathrm{g}} = q''_{\mathrm{R}} = q''_{\mathrm{s}} = q''_{\mathrm{a}} = q'' \tag{7.29}$$

Assuming that T_g and T_a are known and we want an expression for determining q in terms of these temperatures and h, k, and L, we can rearrange the equations and sum them up as follows:

$$q''_g \frac{1}{h_g} = T_g - T_{iR}$$

$$+ q''_R \frac{L_R}{k_R} = T_{iR} - T_{Rs}$$

$$+ q''_s \frac{L_s}{k_s} = T_{Rs} - T_{sa}$$

$$+ q''_a \frac{1}{h_a} = T_{sa} - T_a$$

$$q'' \left(\frac{1}{h_g} + \frac{L_R}{k_R} + \frac{L_s}{k_s} + \frac{1}{h_a} \right) = T_g - T_a \tag{7.30}$$

The heat flux between the gas and ambient air can be calculated from their temperatures only using an expression from electrical resistances, that is, $I = E/R$, as

$$q'' = \frac{T_g - T_a}{\dfrac{1}{h_g} + \dfrac{L_R}{k_R} + \dfrac{L_s}{k_s} + \dfrac{1}{h_a}} = \frac{T_g - T_a}{\Sigma R} \tag{7.31}$$

where ΣR is the thermal resistance for heat transfer between the gas and the ambient air. A similar expression for a composite cylinder shown in Figure 7.5 can be deduced using Equation 7.19 as follows:

$$q'' = \frac{T_g - T_a}{\dfrac{1}{h_g 2\pi r_1} + \dfrac{\ln(r_2/r_1)}{2\pi L k_1} + \dfrac{\ln(r_3/r_2)}{2\pi L k_2} + \dfrac{\ln(r_4/r_3)}{2\pi L k_3} + \dfrac{1}{h_a 2\pi r_4 L}} \tag{7.32}$$

From these we can also define the thermal conductance through the composite wall as $U = 1/RA$, that is, the rate of heat transfer per degree of temperature drop per square meter, from which follows the heat transfer as

$$Q = UA\Delta T \tag{7.33}$$

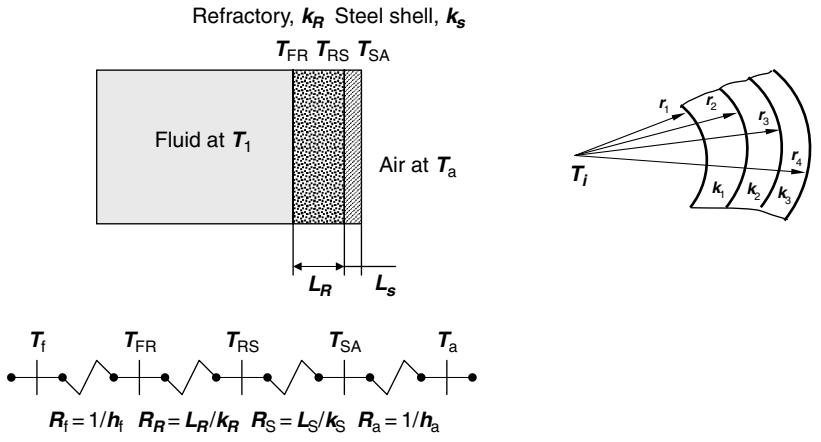

Figure 7.5 Thermal resistances in composite walls.

7.5 Shell Losses

Shell heat loss plays a major role in rotary kiln operation. For some applications such as cement kilns, the shell temperature scans can be one way of controlling the process. Heat losses through the shell can give an indication of what is happening inside the kiln. Even if the kiln is equipped with cameras, refractory failure can only be detected by increased shell temperature at that particular location of failure. Conditions such as these are normally evidenced by hot spots. Some modern cement kiln operations are equipped with temperature scanners that continuously scan the shell and record real time temperature profiles. Any causes that effect temperature changes inside the kiln, for example, increased feed rate, low fuel rate, changes in airflow rate, and so on, will change the shell temperature profile. The drawback in using the shell wall for kiln control is that the refractory lining has a large thermal mass and its response time to temperature change inside the kiln is slow. That is the reason why some operators prefer to use the inside wall temperature as a control point by pointing cameras equipped with temperature sensors (e.g., Micron or Ircon).

7.6 Refractory Lining Materials

The type and thickness of the refractory material used for kiln lining are critical to heat losses through the kiln shell and play a major

role in the design and maintenance of the process. The mechanics of wall-shell heat transfer are treated later. The critical thickness required for a lining to insulate the kiln is a heat transfer problem because beyond a certain threshold it no longer performs as an insulator. The thermal properties of the refractory materials, particularly their thermal conductivity, do control the rate of shell heat loss. Considering that about 25 percent of the total heat loss is through the shell, such losses can dramatically influence process efficiency, fuel efficiency, and lining life.

Materials for refractory lining are chosen based on several factors, including their stability and durability. While the main intention is to protect the steel shell, they can serve as an insulation material necessary to retain the heat within the kiln interior. At the sections near the combustion zone, conductive materials are preferred for lining so as to dissipate some heat away and prevent excessive temperature build-up and thereby avoid thermal stresses and associated refractory damage. Lining materials come in all forms including bricks and mortars of all consistency that can be spread or sprayed on surfaces. The material composition and thermo-physical properties of some lining materials are presented in Table 7.1.

Figures 7.6 and 7.7 are calculated shell losses based on refractory type and thickness. Although the actual mechanism of heat loss through a rotary kiln wall is more involved, the obvious result is that

Table 7.1 Composition and Thermal Properties of Some Refractory Materials Used in Rotary Kilns

	Refractory Type		
Chemical Analysis (Calcined Basis), %	**High Alumina Brick**	**High Alumina Brick**	**Burnt Magnesite (Basic Brick)**
Silica (SiO_2)	24.6	15.2	2.7
Alumina (Al_2O_3)	70.8	78.7	10.9
Titania (TiO_2)	3.0	3.4	0.3
Iron oxide (Fe_2O_3)	1.3	1.8	1.1
Lime (CaO)	0.1	0.3	1.9
Magnesia (MgO)	0.1	0.2	83.1
Alkalies ($Na_2O + K_2O$)	0.1	0.4	—

(*Continued*)

Table 7.1—Cont'd

	Refractory Type		
Chemical Analysis (Calcined Basis), %	**High Alumina Brick**	**High Alumina Brick**	**Burnt Magnesite (Basic Brick)**
Properties			
Bulk density (kg/m^3)	2579	2707	2835
Apparent porosity (%)	17	19.8	19.4
Crushing strength at 21°C (N/mm^2)	45	56	22
Modulus of rupture	10	9	5
Linear change at temperature (%)	+2.0 at 1600°C	+1.2 at 1599°C	0 at 1482°C
Thermal conductivity at temperature (W/m·K)			
at 1000°C	1.78	1.79	2.56
at 1200°C	1.77	1.82	2.47
at 1400°C	1.78	1.85	2.37

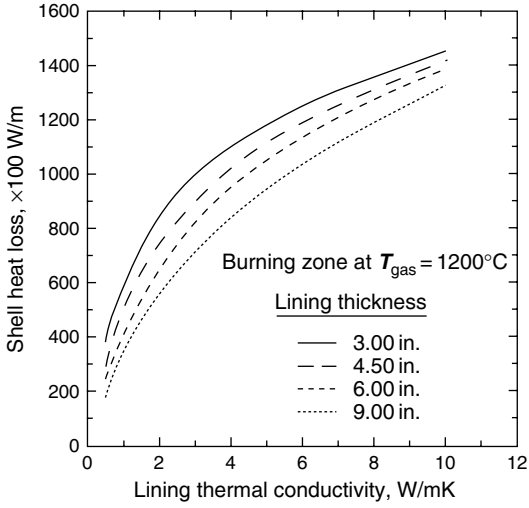

Figure 7.6 Refractory thermal conductivity and shell losses.

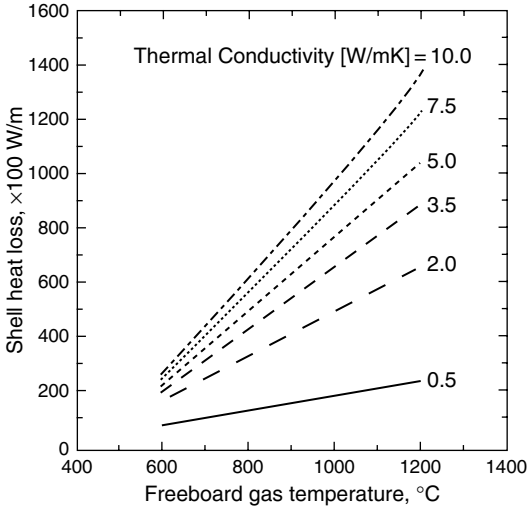

Figure 7.7 Flame temperature and shell losses.

heat loss increases with conductivity and also with reduced refractory thickness. The shell heat losses also depend on the temperature difference between the freeboard and the ambient temperature as is demonstrated in Figure 7.7.

7.7 Heat Conduction in Rotary Kiln Wall

Heat transfer in a rotary kiln wall is composed of heat loss through the freeboard gas or flame to the exposed wall and heat loss from the material being processed to the wall covered with material. Because the wall is rotating, the problem is not that of a steady state heat transfer but a cyclic equilibrium including transient responses. As shown in Figure 7.8, the kiln wall can be divided into two regions: (i) the active layer at the inner surface that undergoes a regular cyclic temperature change as the wall rotates through the freeboard and beneath the bed burden, and (ii) a steady state layer extending from the active region to the outer surface, which does not experience any temperature variation as a function of kiln rotation.

The governing equation for heat conduction in the cross section of a rotating wall can be approximated by that of transient heat conduction in spherical coordinates as (Gorog et al., 1982)

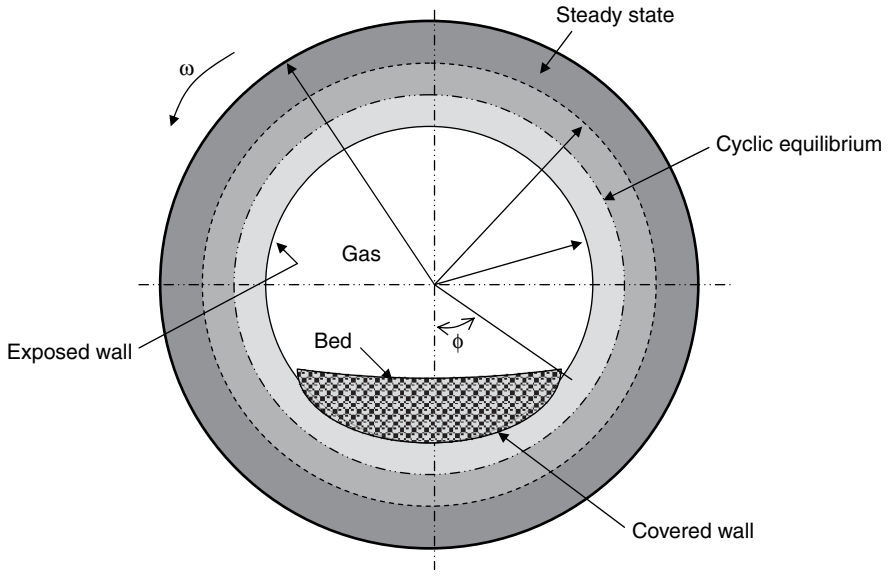

Figure 7.8 Cross sectional view of heat conduction through rotary kiln wall.

$$\frac{\partial}{\partial r}\left(k_{\mathrm{w}}\frac{\partial T_{\mathrm{w}}}{\partial r}\right)+\frac{k_{\mathrm{w}}}{r}\frac{\partial T_{\mathrm{w}}}{\partial r}+\frac{1}{r^2}\frac{\partial}{\partial \phi}\left(k_{\mathrm{w}}\frac{\partial T_{\mathrm{w}}}{\partial \phi}\right)+\frac{\partial}{\partial z}\left(k_{\mathrm{w}}\frac{\partial T_{\mathrm{w}}}{\partial z}\right)=\rho_{\mathrm{w}}c_{p_{\mathrm{w}}}\frac{\partial T_{\mathrm{w}}}{\partial t} \tag{7.34}$$

It can be assumed that heat conduction in the longitudinal and the circumferential directions are negligible, that is,

$$\frac{\partial T_{\mathrm{w}}}{\partial z}=\frac{\partial T_{\mathrm{w}}}{\partial \phi}=0 \tag{7.35}$$

For $R_i \le r \le R_{\mathrm{f}}$, that is, in the active region

$$\frac{\partial^2 T_{\mathrm{w}}}{\partial r^2}+\frac{1}{r}\frac{\partial T_{\mathrm{w}}}{\partial r}=\frac{1}{\alpha_{\mathrm{w}}}\frac{\partial T_{\mathrm{w}}}{\partial t} \tag{7.36}$$

with the following boundary conditions

1. At the inner surface of the exposed wall, for $0 \le \phi \le 2(\pi - \phi_L)$ and $t > 0$,

$$-k_{\mathrm{w}}\frac{\partial T_{\mathrm{w}}}{\partial r}\bigg|_{r=\mathrm{Ri}}=h_{\mathrm{g}\to\mathrm{ew}}(T_{\mathrm{g}}-T_{\mathrm{w}})$$

2. At the covered wall, for $2(\pi - \phi_L) < \phi_L < 2\pi$ and $t > 0$,

$$-k_{\mathrm{w}} \left.\frac{\partial T_{\mathrm{w}}}{\partial r}\right|_{r=\mathrm{Ri}} = h_{\mathrm{ch}\to\mathrm{cw}}(T_{\mathrm{b}} - T_{\mathrm{w}})$$

3. At the interface between the two regions, for $r = R_{\mathrm{f}}$, $0 \le \phi \le 2\pi$, and $t > 0$,

$$T_{\mathrm{w}} = T_{\mathrm{f}}$$

For the steady-state region, that is, $R_{\mathrm{f}} \le r \le R_0$, Equation (7.34) reduces to

$$\frac{\partial^2 T_{\mathrm{w}}}{\partial r^2} + \frac{1}{r}\frac{\partial T_{\mathrm{w}}}{\partial r} = 0 \tag{7.37}$$

With a boundary condition for $0 \le \phi \le 2\pi$,

$$-k_{\mathrm{w}} \left.\frac{\partial T_{\mathrm{w}}}{\partial r}\right|_{r=\mathrm{R}_0} = h_a(T_{sh} - T_a)$$

The solution of Equations (7.36) and (7.37) with their respective boundary conditions gives temperature distribution for the steady state region as

$$T_{(r)} = T_{\mathrm{f}} - \frac{T_{\mathrm{f}} - T_a}{\ln\left(\dfrac{R_0}{R_{\mathrm{f}}}\right) + \dfrac{k_w}{h_a R_0}} - \ln\left(\frac{r}{R_{\mathrm{f}}}\right) \tag{7.38}$$

For the transient region the reader is referred to any heat transfer text for Heisler charts. Alternately, the transient region can be solved numerically by first guessing the location of the interface and iterating the procedure until the heat loss between the cyclic equilibrium region equals that of the steady state region. The heat transfer coefficients include that of convection and radiation, which we will evaluate after treating radiative heat transfer.

7.8 Radiation Heat Transfer

Heat transfer by thermal radiation requires no intervening medium. Thermal radiation is the energy emitted by a body solely due to the temperature of the body and at a frequency that falls within a small portion of the electromagnetic wave spectrum as shown in Figure 7.9.

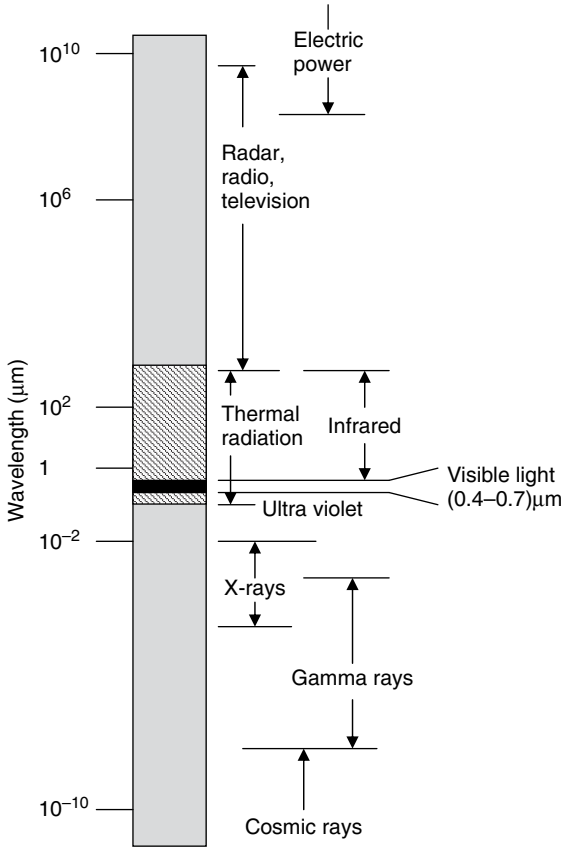

Figure 7.9 The electromagnetic wave spectrum.

7.8.1 The Concept of Blackbody

When radiation is incident on a homogeneous body, some of it is reflected and the remainder penetrates into the body. The radiation may then be absorbed as it travels through the medium. When the dimensions, that is, the thickness allows transfer of energy such that some of the radiation is transmitted through the body, then the transmitted radiation will emerge unchanged. If the material is a strong internal absorber then the radiation that is not reflected from the body will be converted into internal energy within the layer near the surface. To be a good absorber for incident energy, a material must have a low surface reflectivity and sufficiently high internal absorption to prevent the radiation from passing through it. A surface is said to be

radiatively "black" when it has zero surface reflection and complete internal absorption. A hypothetical blackbody is defined as an ideal body that allows all the incident radiation to pass into it (no reflected energy) and absorbs internally all the incident radiation (no transmitted energy). This is true for radiation for all wavelengths and for all angles of incidence. Hence a blackbody is a perfect absorber of incident radiation and in radiation heat transfer serves as the standard with which real absorbers can be compared. The Stefan Boltzmann Law states that the total (hemispherical) emissive power of a blackbody is proportional to the fourth power of the absolute temperature

$$E_{\mathrm{b}} = \sigma T^4 \left[\frac{\mathrm{W}}{\mathrm{m}^2}\right] \tag{7.39}$$

where a hemispherical surface is defined as one that embodies all directions of the half space. So therefore, the total emissive power of a real surface can only be a ratio of the blackbody. This ratio is defined by the emissivity $\varepsilon = E/E_{\mathrm{b}}$ of the body

$$E = \varepsilon E_{\mathrm{b}} = \varepsilon \sigma T^4 \left[\frac{\mathrm{W}}{\mathrm{m}^2}\right] \tag{7.40}$$

This total emissive power includes all wavelengths within the thermal energy band. However, even a blackbody does not emit equally at all wavelengths. The blackbody emissive power at a particular wavelength is called the monochromatic emissive power and is related to the wavelength and temperature according to Plank's Law as

$$E_{\mathrm{b},\lambda} = \frac{C_1 \lambda^{-5}}{e^{C_2/\lambda T} - 1} = f(\lambda, T) \left[\frac{W}{\mathrm{m}^2 \mathrm{m}}\right] \tag{7.41}$$

where $C_1 = 3.742 \times 10^{-16}$ [W/m^2] and $C_2 = 1.439 \times 10^{-2}$ [mK]. Therefore plots of $E_{\mathrm{b},\lambda}$ indicate that as the temperature of the blackbody increases the maximum monochromatic emissive power shifts to shorter wavelengths leading to Wein's Displacement Law which states that the product of the temperature and the wavelength must be a constant, that is, $\lambda_{\max} T = 2.898 \times 10^{-3}$. The relationship was derived by solving Plank's Law for $\left(\frac{\mathrm{d}E_{\mathrm{b},\lambda}}{\mathrm{d}\lambda}\right)_T \to 0$. Similarly, real surfaces do not emit with equal efficiency at all wavelength hence one can define a monochromatic emissivity as $\varepsilon_\lambda = E_\lambda / E_{\mathrm{b},\lambda}$ leading to an idealized "gray" surface for which $\varepsilon_\lambda = \varepsilon = const.$

7.9 Radiation Shape Factors

We have said earlier that the cylindrical enclosure of the rotary kiln maximizes radiation heat transfer in the freeboard. This is due to the fact that radiation exchange is geometry dependent. A fundamental problem in radiation heat transfer is estimating the net radiant exchange between surfaces. One can define the total energy streaming away from a surface as the *radiosity* and the energy incident on a surface as the *irradiation*. Figure 7.10 illustrates the concept whereby the surface is emitting its own energy at a rate E and is also reflecting energy incident on the surface or part of the irradiation G at a rate, ρG, where ρ is the reflectivity. The total energy leaving the surface, that is, the radiosity, J, is

$$J = E + \rho G = \varepsilon E_b + \rho G \tag{7.42}$$

where ε is the surface emissivity. If a number of surfaces i are involved in radiation exchange, each surface has a radiosity J_i. For non-diffuse surfaces, J_i will depend on the direction of the radiation as well.

One can derive the net radiative exchange between two surfaces separated by a nonabsorbing medium by considering Figure 7.11 which shows elemental areas dA_1 and dA_2 that form portions of the finite areas A_1 and A_2. If we define I_1 as the net intensity of radiation leaving surface 1 in the direction θ_1, then the total energy intercepted by surface dA_2 is

$$dE_{1\to 2} = I_1 dA_1 \cos\theta_1 d\omega_1, \quad d\omega_1 = dA_2 \cos\theta_2 / r^2 \tag{7.43}$$

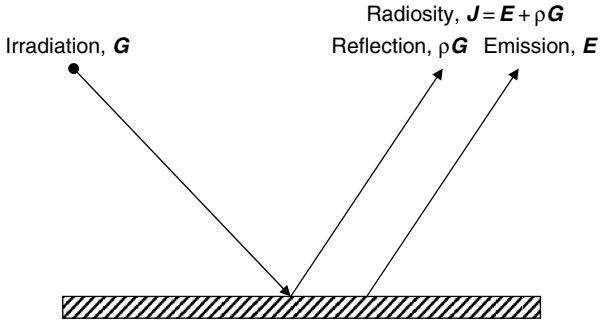

Figure 7.10 The concept of radiosity and irradiation.

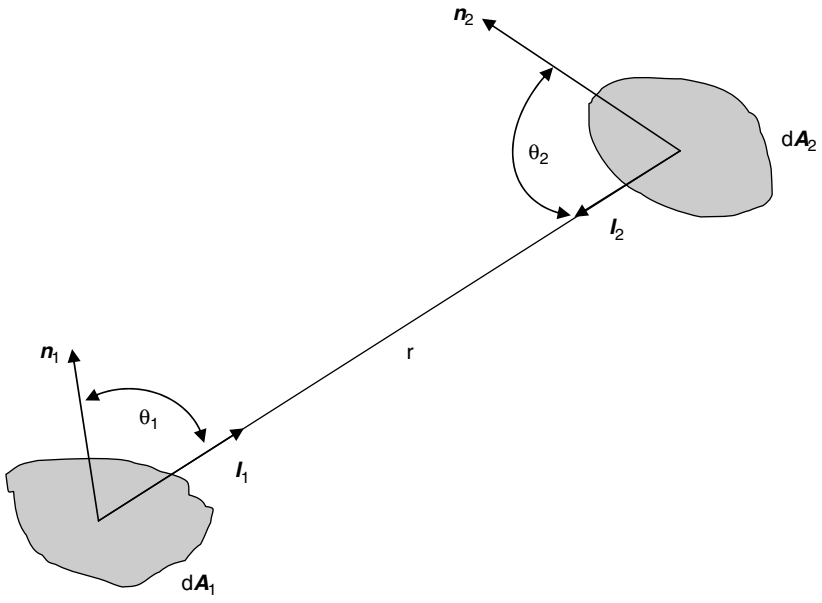

Figure 7.11 Radiation view factor.

The total energy leaving surface I is

$$dE_1 = dA_1 \left[2\pi \int_0^{\pi/2} I_1(\theta) \sin\theta (\cos\theta)\, d\theta \right] \tag{7.44}$$

The ratio of Equations (7.43) and (7.44) is what is known as the shape factor. It is also known as the geometric view factor, configuration factor, or angle factor $dF_{1\to 2}$, and is the fraction of the total radiation leaving surface 1 that is intercepted by surface 2

$$dF_{1\to 2} = dE_{1\to 2}/dE_1 \tag{7.45}$$

View factor analysis is greatly simplified by assuming that both surfaces are diffuse, that is, both radiant intensities I_1 and I_2 are independent of θ_1 and θ_2 which implies that $I_1 = J_1/\pi$ and $dE_1 = J_1 dA_1$. Then Equation (7.45) becomes

$$dF_{dA_1\to dA_2} = \frac{\cos\theta_1 \cos\theta_2}{\pi r^2} dA_2 \tag{7.46}$$

$$dF_{dA_2\to dA_1} = \frac{\cos\theta_2 \cos\theta_1}{\pi r^2} dA_1 \tag{7.47}$$

The reader is referred to heat transfer texts for evaluation of the view factors for specific surfaces and enclosures (Siegel and Howell, 1981; White, 1988).

7.10 Radiation Exchange Between Multiple Gray Surfaces

As Equation (7.45) indicates, knowledge of the view factor allows for the calculation of the net radiation between any two blackbodies as

$$Q(net)_{1\to 2} = A_1 F_{1\to 2}\sigma\left(T_1^4 - T_2^4\right) \tag{7.48}$$

For non-black surfaces, the net interchange must account for the reflected radiant energies from other surfaces. For refractory material surfaces encountered in rotary kilns, perhaps one can assume that all surfaces are gray, diffuse, and opaque, that is,

$$\tau = 0, \quad \alpha = \varepsilon, \quad \rho = 1 - \varepsilon \tag{7.49}$$

Hence, knowledge of the emissivity completely characterizes the surface. Of course, non-gray and non-diffuse surfaces bring several degrees of complication into the calculations. By employing the concept of radiosity and irradiation illustrated in Figure 7.10, the net thermal radiation heat exchange between surfaces i can be computed by

$$Q_i = A_i\left(J_i - G_i\right) \tag{7.50}$$

Substituting J_i from Equation (7.42) and ρ_i from Equation (7.49) gives

$$Q_i = \frac{\varepsilon_i A_i}{1-\varepsilon_i}\left(E_{bi} - J_i\right) \tag{7.51}$$

Equation (7.51) can be interpreted either algebraically or electrically as was done for Newton's Law of cooling in convection or for Fourier's Law of conduction through composite materials. The electrical analogy for Equation (7.51) can be made by comparing $(E_{bi} - J_i)$ to the driving potential difference and Q_i as the electrical current.

$$Q_i = \frac{E_{bi} - J_i}{R_i} \qquad R_i = (1-\varepsilon_i)/(\varepsilon_i A_i) \tag{7.52}$$

where R_i is the radiative resistance of the gray surfaces. Similarly, the shape factor relation between surfaces in Equation (7.48) can be interpreted as

$$Q\,(net)_{1\to 2} = \frac{\left(T_1^4 - T_2^4\right)}{R_{12}} \qquad R_{12} = \frac{1}{A_1 F_{1\to 2}\sigma} \tag{7.53}$$

where R_{12} is a "shape" or "view" resistance between the two surfaces. With the help of the electrical analogy, all the three heat transfer modes (conduction, convection, and radiation) can be linked into an electrical network to calculate the net heat transfer in an enclosure.

7.11 Radiative Effect of Combustion Gases

The term emissivity relates the radiant ability of a surface to the actual temperature of the surface. Because of the formation of radiatively emitting gaseous products of combustion, especially CO_2 and H_2O, all hydrocarbon flames produce significant levels of radiative heat transfer. Also, the presence of particles in a flame can enhance radiative transfer on account of emission from these particles. Flame luminosity is primarily associated with soot particle emission. Flames that do not contain particulates or do not generate significant levels of carbon by pyrolysis, for example natural gas flames, are invisible, while those with high levels of carbon loading, for example coal and oil, are clearly visible. The flame shape, color, emissivity, and temperature together with bed movement will determine the effectiveness of heat transfer from the flame to the bed.

It was mentioned earlier that over 90 percent of the heat transfer in the rotary kiln is by radiation. It is not surprising, therefore, that natural gas, despite its high energy content (about 44–48 MJ/kg), does not sustain heat as effectively as coal (with 23–28 MJ/kg) in kilns. Most of the constituents in liquid waste fuels used in kilns are solvents and alcohols that contain a low carbon-hydrogen ratio. This therefore produces barely visible flames which have low radiant energy emission. It is not uncommon for the kiln operator to face a situation where the measured energy content of such fuels would be high but cannot produce a quality product even when it is possible to increase fuel flow rate within compliance limits.

In modeling the radiative heat transfer from flames, the emissivity and absorptivity of combustion gases are usually represented by the

weighted gray gas mixture model first developed by Hotel (Guruz and Bac, 1981; Jenkins and Moles, 1981). This stems from the fact that gases having a dipole moment (e.g., CO_2, CO, H_2O, and hydrocarbons) are selective absorbers and emitters of radiation, that is, they absorb and emit radiation only within certain wavelengths and this selectivity varies with the gas temperature, pressure, and the geometric shape. Gray gases absorb and emit the same fraction of energy at each wavelength. Hottel and Sarofim (1967) have shown that the emissivity and absorptivity of an equimolar CO_2—H_2O mixture, each with a partial pressure of 11.65 kPa, can be represented as a series of one "clear" where the gray gas absorption coefficient is zero ($K_1 = 0$) and three nonzero gray gases (K_2, K_3, K_4). The absorptivity and emissivity are related to the temperature and wavelength as

$$\varepsilon_g\left(T_g\right) = \sum_{n=1}^{4} a_n\left(T_g\right)\left[1 - \exp\left(-K_n pL\right)\right] \tag{7.54}$$

$$\alpha_g\left(T_g\right) = \sum_{n=1}^{4} b_n\left(T_s\right)\left[1 - \exp\left(-K_n pL\right)\right] \tag{7.55}$$

where the gray gas absorption coefficients are treated as independent of temperature but the weighting factors are temperature dependent.

7.12 Heat Transfer Coefficients for Radiation in the Freeboard of a Rotary Kiln

Several models exist for estimating the radiative heat transfer in kiln enclosures based, in part, on some of the theoretical foundations presented herein (Barr et al., 1989; Boateng and Barr; 1996; Gorog et al., 1981; Gorog et al., 1983; Guruz and Bac, 1981; Jenkins and Moles, 1981; and others). Almost all of these follow the zone model of Hotel and Cohen (1958) whereby models for calculating radiative exchange within enclosures are constructed by subdividing the enclosure, including the gas contained within, into numerous zones and then formulating the expressions for radiative exchange among the zones. What is different among the several radiation models presented by the various authors is the tools used for the solution of the large number of algebraic equations that result from the large number of zones involved in practical combustion chambers, for example, large rotary kilns. While the early researchers used a statistical solution

approach such as the Monte Carlo method to simulate the radiative interchange (e.g., Guruz and Bac, 1981), the advent of high-speed computers have made it possible to apply such models through their inclusion in CFD modeling. We will follow a model by Barr et al. (1989) and Boateng (1993) to illustrate the estimation of the radiative heat transfer coefficients in the rotary kiln enclosure.

The radiant heat transfer between the freeboard gas and the kiln enclosure occurs by the exchange mechanism shown in Figure 7.12.

Radiant heat is transferred either from the gas volume composed of emitting products of combustion, that is, CO_2 and H_2O, or by particulate emission in the freeboard region to the bed surface, $Q_{g\text{-}eb}$, or to the exposed wall, $Q_{g\text{-}ew}$. The wall (refractory lining) interacts radiatively with the bed with radiative heat transfer, $Q_{eb\text{-}ew}$. In addition, some sections of the wall do exchange radiant energy with other sections of the wall once the enclosure is such that they see each other. Only a portion of the energy absorbed by the inside wall (refractory) surface during exposure to freeboard gas is lost through the outer shell (by conduction) of the refractory lining. The remainder is transferred to the bottom of the bed (regenerative heat transfer).

Calculations of radiative exchanges are carried out by tracing individual beams of radiation from their source to the surface of interest.

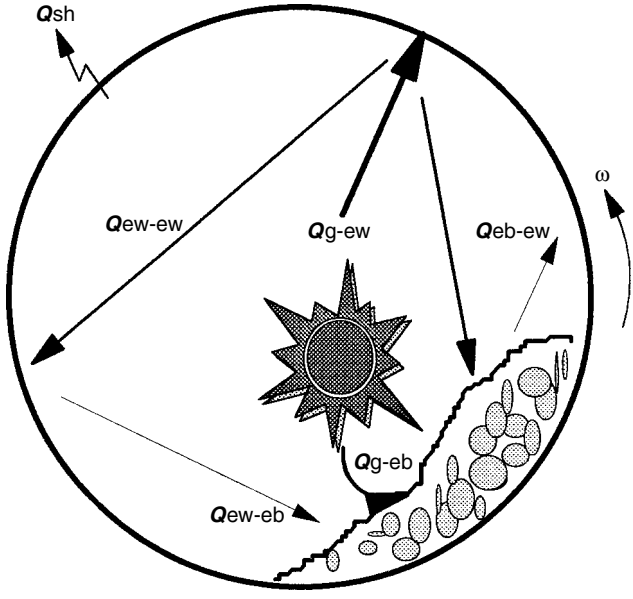

Figure 7.12 Radiant heat transfer paths.

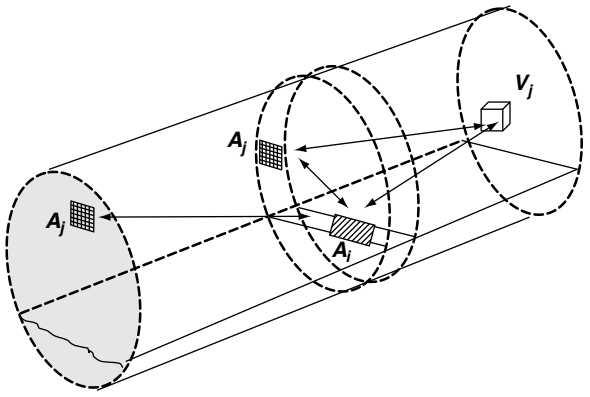

Figure 7.13 Radiative exchange in the axial zones.

The circumferential strip of the kiln freeboard (Figure 7.13) is isolated and subdivided in N small area elements. The portion of the kiln freeboard, approximately three kiln inside diameters in each axial direction viewed by these area elements, is subdivided into volume zones such as V_j comprising the freeboard gas, and the surface zones such as A_j that form the exposed bed and wall surfaces. The exchange areas between each of the zones and the elements of the circumferential strip are then evaluated and used to calculate the radiation streaming to these elements from the various volumes and surface zones, either directly or after undergoing one or two reflections.

7.13 Radiative Exchange from the Freeboard Gas to Exposed Bed and Wall Surfaces

Radiative exchange between elements A_i (exposed bed) or refractory wall and the gas volume V_j is calculated by using the expression for gray surfaces.

$$Q_{V_j \leftrightarrow A_i} \approx \frac{\varepsilon_i + 1}{2} \sum_{n=1}^{4} \left(g_j s_i\right)_n \left(E_j - E_i\right)_n \tag{7.56}$$

Equation (7.56) accounts for the irradiation of the surface elements by the contribution of each component of the gas emissivity. Barr et al. (1989) found that for a rotary pilot kiln of about 40 cm diameter and 3.5 m long, more that 80 percent of reflected gas radiation leaving a surface was reabsorbed by the freeboard gas without impinging on

another surface. Hence the effect of reflections could be ignored to simplify the calculations. The freeboard viewed by elements A_i can be considered as two symmetric regions one upstream and the other downstream. The geometrical exchange areas $g_j s_i$ can be calculated for one region and take advantage of the symmetry to further simplify the model. The net radiative heat transfer computed by summing up Equation (7.56) over the subdivided volume zones is

$$Q_{g\leftrightarrow A_i} = \frac{\varepsilon_i + 1}{2} \sum_{j=1}^{N} \sum_{n=1}^{4} \left(g_j s_i\right)_n \left(E_j - E_i\right)_n \tag{7.57}$$

where N is the number of zones or volume elements typically greater than 300. Like any computational domain, the larger the number of divisions N, the better the accuracy of the computations.

7.14 Radiative Heat Transfer among Exposed Freeboard Surfaces

The direct radiation exchange between a freeboard surface zone such as A_j and an area element A_i, that is, exposed wall-to-exposed bed on the circumferential strip may be calculated using the expression

$$Q^0_{A_j\leftrightarrow A} = \sum_{n=1}^{4} \left(s_j s_i\right)_n \left(\varepsilon_j \varepsilon_i E_j - \varepsilon_i \varepsilon_j E_i\right)_n \tag{7.58}$$

The energy streaming between A_i and A_j must traverse the intervening freeboard gas hence the view factors $(s_j s_i)$ must be computed first. For surface emissivities less than 0.9, which is the case for refractory and bed surfaces, reflectivity can be significant. To account for the reflected energy in the interchange one can simplify the calculation by assuming a single reflection from the intermediate surfaces or multiple reflections depending on the accuracy of interest. For a single reflection depicted in Figure 7.14, the net radiative exchange between the element A_i and zone A_i involving a single reflection from an intermediate surface A_k can be expressed as

$$Q_{A_j\leftrightarrow A_k\leftrightarrow A_i} = \sum_{n=1}^{4} \varepsilon_i \varepsilon_j \rho_k \left(s_j s_k\right)_n \frac{\left(s_k s_i\right)_n}{A_k} \left(E_j - E_i\right)_n \tag{7.59}$$

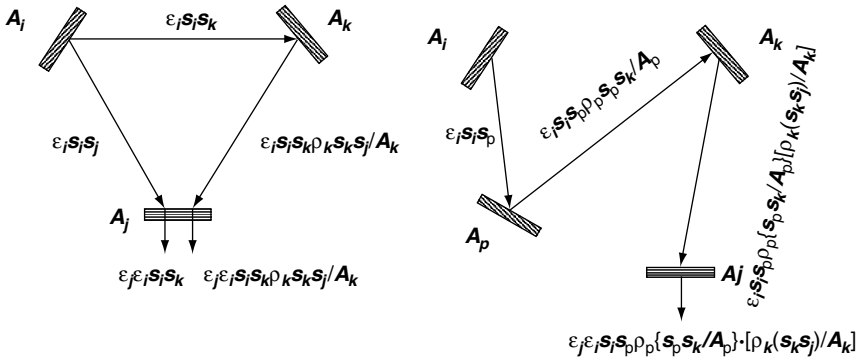

Figure 7.14 Radiative exchange with reflectivity.

By summing over all the reflecting surfaces, an expression for the radiative exchange between A_i and A_j involving a single reflection is obtained as

$$Q^1_{A_j \leftrightarrow A_i} = \sum_{all-k} Q_{A_j \leftrightarrow A_k \leftrightarrow A_i} \tag{7.60}$$

Extending the analysis to include an additional reflection will yield a net radiative exchange between A_i and A_j as

$$Q_{A_j \leftrightarrow A_i} = Q^0_{A_j \leftrightarrow A} + Q^1_{A_j \leftrightarrow A_i} + Q^2_{A_j \leftrightarrow A_i} \tag{7.61}$$

Barr et al. (1989) found that the error introduced by accounting for only two reflections was only 3 percent in pilot rotary kilns except the lining material is such that the emissivity is below 0.5. For large rotary kilns, an emissivity of 0.7 is typical for the refractory walls.

For the process or kiln engineer perhaps the important application is to develop a catalog of radiative heat transfer coefficients, which can be combined with convection heat transfer coefficients to estimate the kiln heat balance. Cognizant of the fact that the radiative exchange between an area element and any zone in the freeboard is a function of temperature, pressure, and geometry, the radiative heat transfer coefficient can be cast into the form

$$h_{V_j \rightarrow A_i} = \frac{Q_{V_j \leftrightarrow A}}{A_i (T_j - T_i)} \tag{7.62}$$

Barr et al. (1989) employed the equations presented herein to assemble the radiative heat transfer coefficients for the entire freeboard gas,

that is, $h_{g\rightarrow ewi}$, and $h_{g\rightarrow ebi}$, the entire exposed bed surface, $h_{eb\rightarrow ewi}$, and the entire exposed wall, $h_{ew\rightarrow ewi}$. Some radiative heat transfer coefficients from the freeboard gas to the participating surfaces are presented in Figures 7.15–7.17 for a 41 cm diameter pilot kiln (Barr et al., 1989).

These show that except near the corners formed by the exposed bed and wall, both $h_{g\rightarrow ewi}$ and $h_{g\rightarrow ebi}$ are nearly uniform and for all practical reasons can be replaced by one averaged value for both coefficients. As implied by Equations (7.54) and (7.55) $h_{eb\rightarrow ew}$ varies with the partial pressure and with the temperature difference between the gas and the participating surface, that is, the driving potential as per the electrical analogy. Calculations show that for larger kilns, for example, 4 m diameter kilns at the same operating conditions, these coefficients can be an order of magnitude greater than for the pilot kilns essentially due to the geometric view factors. What can also be deduced from the plots is the effect of freeboard gas temperature, T_g, on the magnitude of the exposed wall heat transfer coefficient, that is, h_{ew} increases with increased freeboard gas temperature. The regenerative action of the wall may see a temperature variation at the inside face showing that as the kiln rotates, the wall will pick up energy from the freeboard gas and will give it to the bed at the covered wall. Aside from the

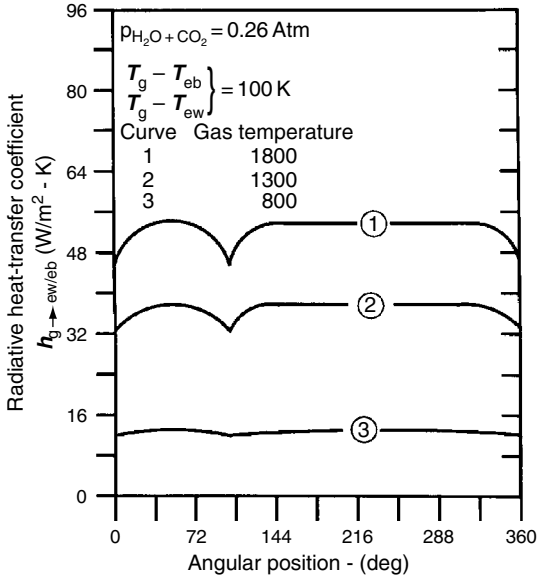

Figure 7.15 Predicted radiation heat transfer coefficients from freeboard gas to the exposed wall for a 41 cm diameter pilot kiln (Barr et al., 1989).

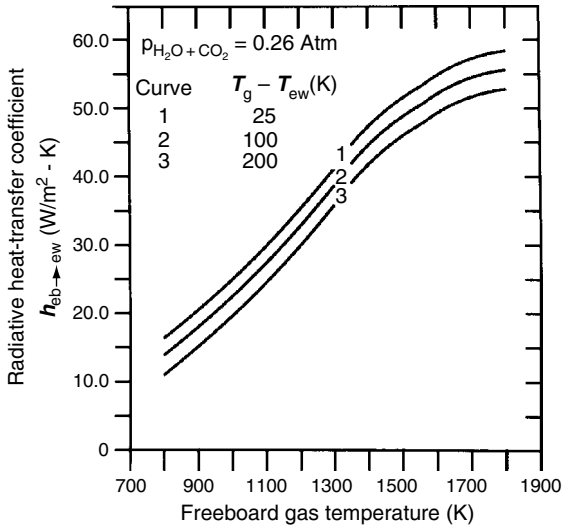

Figure 7.16 Radiative heat transfer coefficient from exposed bed to exposed wall as a function of gas-to-wall temperature difference (Barr et al., 1989).

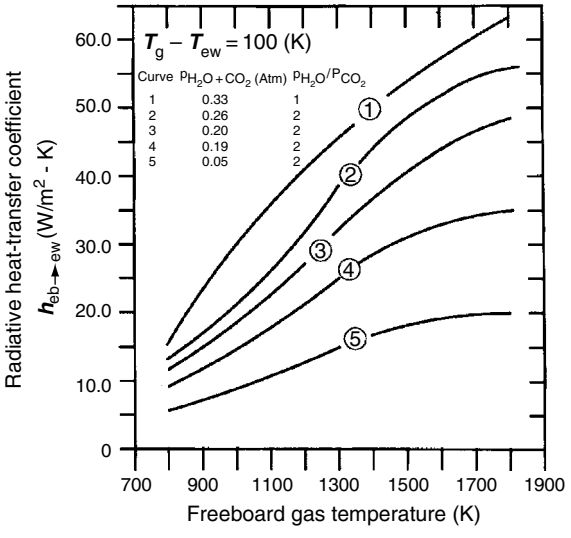

Figure 7.17 Radiative heat transfer coefficient from exposed bed to exposed wall as a function of emitting gas partial pressure (Barr et al., 1989).

regenerative effect, the thickness of the wall active region depends on the freeboard gas temperature. The modeling of the bed heat transfer will be covered in detail in Chapter 8.

References

P. V. Barr, J. K. Brimacombe, and A. P. Watkinson. "A heat-transfer model for the rotary kiln: Part II. Development of the cross-section model," *Met. Trans. B*, 20, 403–419, 1989.

A. A. Boateng. *Rotary Kiln Transport Phenomena: Study of the Bed Motion and Heat Transfer*, PhD Dissertation, The University of British Columbia, Vancouver, 1993.

A. A. Boateng and P. V. Barr. "A thermal model for the rotary kiln including heat transfer within the bed," *Int. J. Heat Mass Transfer*, 39(10), 2131–2147, 1996.

J. P. Gorog, J. K. Brimacombe, and T. N. Adams. "Radiative heat transfer in rotary kilns," *Met. Trans. B*, 12, 55–69, 1981.

J. P. Gorog, T. N. Adams, and J. K. Brimacombe. "Regenerative heat transfer in rotary kilns," *Met. Trans. B*, 13(2), 153–163, 1982.

J. P. Gorog, T. N. Adams, and J. K. Brimacombe. "Heat transfer from flames in a rotary kiln," *Met. Trans. B*, 14(3), 411–423, 1983.

H. K. Guruz and N. Bac. "Mathematical modelling of rotary cement kilns by the zone method," *Can. J. Chem. Eng.*, 59, 540–548, 1981.

H. C. Hottel and A. Sarofim. *Radiative Heat Transfer*. McGraw-Hill, New York, 1967.

H. C. Hottel and E. S. Cohen. "Radiant heat exchange in a gas-filled enclosure: Allowance for nonuniformity of gas temperature," *AIChE J.*, 4(1), 3–14, 1958.

B. G. Jenkins and F. D. Moles. "Modelling of heat transfer from a large enclosed flame in a rotary kiln," *Trans. IChemE*, 59, 17–25, 1981.

R. Siegel and J. R. Howell. *Thermal Radiation Heat Transfer*. McGraw-Hill, New York, 1981.

F. White. *Heat and Mass Transfer*. Addison-Wesley, New York, 1988.